Bumpless Transfer of Non-inverting Buck Boost Converter among Multiple Working Modes

Jianjun MA, *Student Member*, *IEEE*, Miao ZHU, *Senior Member*, *IEEE*, Xiuyi LI, Xu CAI
School of Electronic Information and Electrical Engineering, Shanghai Jiao Tong University, China
(mjjamazon@sjtu.edu.cn, miaozhu@sjtu.edu.cn)

***Abstract*—In dealing with the wide operation voltage of renewable energy and energy storage devices, Non-inverting buck-boost converter (NIBB) has been utilized for DC-DC power conversion. This converter shows high efficiency with multi-mode operation. However, transition among multiple working modes will inevitably introduce the "voltage bump", thus hindering the performance of power converter. In this paper, the cause of voltage bump is first revealed. In elimination of the voltage bump, an *improved buck/boost mode* is introduced as transition mode, and *current feed-forward compensation* has been proposed. The combined method is evaluated against classical solutions and verified through the gradual improvement of control performance.**

I. INTRODUCTION

Both renewable energy sources (RES) [1] and energy storage devices [2] exhibit a wide range of output voltage, fluctuating with particular working condition. When they are connected with DC-DC converter for power conversion, input voltage range often intersects with output voltage range. For interlinking converter between DC micro-grids [3], both input and output voltages vary according to system power status. In all these cases [1]-[6], the power converter working in wide operation range, both voltage step-up and step-down capability is required.

Classical DC-DC converters [7] such as buck, boost converter, feature single control input. When they are operating with wide input voltage, the duty ratio will also vary in large range, making it difficult for performance optimization. In contrast, NIBB, as shown in Fig.1, offers multiple modes to cope with wide conversion range. In *Buck mode*, S_2 is constantly on, only S_1 and S_3 switching in each cycle; in *Boost mode*, S_1 is constantly on, only S_2 and S_4 switching in each cycle. Considering the maximum switch duty ratio, *transition mode* is also needed between *Buck* and *Boost mode* to attain continuous voltage conversion ratio.

Although the multiple modes offer more flexibility, it also poses new challenges. When the input voltage v_I varies, NIBB works across different mode, and different combinations of control variables (d_1, d_2) present alternatively, indicating the change of open-loop dynamic property. Since each mode has its' corresponding dynamic model, the close loop controller should be designed for each mode separately [9]-[10]. When working mode changes, not only the open loop dynamic model change, the close loop controller will also vary.

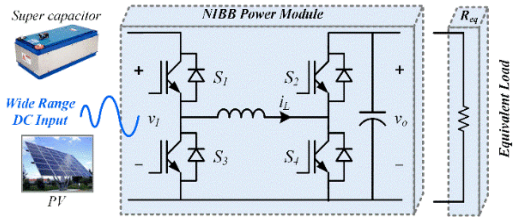

Fig.1 Circuit of Multi-mode Buck Boost Converter

From the above analysis, multi-mode operation of NIBB involves "design of working modes" (particularly the *Transition mode*) and "transfer between multiple controllers". In previous researches, the only design criterion of *Transition mode* is converter efficiency [4]. The dynamic influence of mode transition is treated as disturbance and often ignored. Besides, few literatures cover the detailed transfer method between multiple controllers. Although the classical control theory [8] provides some insights on bumpless control design, that is not enough for operation of NIBB, which will be shown below.

There lacks a closer examination on the effect caused by mode transition and the solutions, this paper serves to fill the gap. Organization of the paper is given as follows: a review of multi-mode operation of NIBB is given in section II. In Section III, the voltage bump caused by mode transition is evaluated with the defined large-signal index. In section IV, bumpless control with feed-forward compensation is introduced. The proposed operation strategy is evaluated and compared with the classical solutions in Section V.

II. REVIEW ON MULTI-MODE OPERATION OF NIBB

As a basis for the following analysis, average model of NIBB can be derived as:

$$\begin{cases} L\dfrac{di_L}{dt} = d_1 v_i - d_2 v_o \\ C\dfrac{dv_o}{dt} = d_2 i_L - \dfrac{v_o}{R_{eq}} \end{cases} \tag{1}$$

Where, d_1 and d_2 are duty ratio of S_1 and S_2 respectively. The steady-state value can be attained by setting the differential term to 0. The steady-state voltage conversion ratio is given by:

$$\frac{V_o}{V_i}=\frac{D_1}{D_2} \tag{2}$$

An illustrative representation of voltage conversion ratio is slope of the line connecting "O" and the working point, as is shown in Fig.2. For practical power switch, due to the presence of dead time, there exist a maximum duty ratio D_{max} and minimum duty ratio D_{min}, The resulting operation area of NIBB can be presented as A_1A_2, B_1B_2, as well as **σ**.

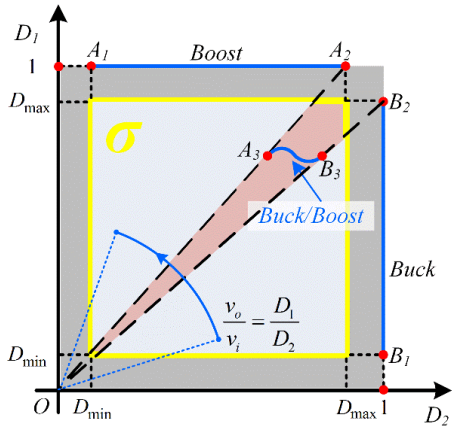

Fig.2 Operation area of NIBB

As is shown in Fig.2, operation of NIBB covers multiple modes [4]-[6]. In A_1A_2 (*Boost mode*), S_1 is constantly closed, NIBB works exactly as Boost converter. In B_1B_2 (*Buck mode*), S_2 is constantly closed, NIBB works exactly as Buck converter. *Boost* and *Buck modes* are not enough to ensure continuous voltage conversion, thus a gap shown as A_2OB_2 will present. Since practical input/output voltage varies continuously, this gap will lead to increase sub-harmonics and instability if uncontrolled.

To ensure continuous voltage conversion, the converter will work within σ, or A_2OB_2, to be more specific. Theoretically, any line connecting A_3 on OA_2 and B_3 on OB_2 can be taken as transition mode. Lots of publications have proposed different transition modes [9], [10]. In fact, any A_3 on OA_2 and any B_3 on OB_2 can serve for continuous voltage conversion. While different combinations of A_3 and B_3 will introduce different transition mode.

Although both A_2 and A_3 have the same voltage conversion ratio, dynamic property at the two working points are inherently different. With the increase of v_o/v_i, NIBB will work through B_1B_2 (*Buck mode*), B_3A_3(*Buck/Boost mode*) and A_2A_1(*Boost mode*). To avoid the possible mode chattering caused by noise, a small hysteresis [5] can be inserted between A_2, A_3 and A_5, A_6. The resulting mode switching logic is shown in Fig.3.

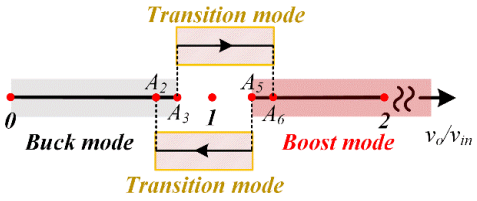

Fig.3 Logic of mode switching

With the increase or decrease of v_o/v_i, only one specific combination of d_1 and d_2 presents for one given voltage conversion ratio. Therefore, equivalent duty ratio d_{eq} can be introduced to decrease the number of control variables and to simplify NIBB as classical converter which engineers are more familiar with. For ease of implementation, a piecewise linear relation can be defined as:

$$\begin{cases} d_1 = k_1 d_{eq} + c_1, d_2 = 1 \ (d_{eq} < d_{buck}) \\ d_1 = k_2 d_{eq} + c_2, d_2 = k_3 d_{eq} + c_3 \ (d_{buck} \le d_{eq} < d_{boost}) \\ d_1 = 1, d_2 = k_4 d_{eq} + c_4 \ (d_{boost} \le d_{eq}) \end{cases} \tag{3}$$

Based on d_{eq} defined above, the close-loop control will be designed for each mode separately in the same way as classical DC/DC converter.

In this section, a general framework for control design of NIBB with multiple working mode is introduced. It can also be found in existing literature [4]-[6]. The unanswered problems regarding mode transition are as follows:

- How to evaluate effect of mode transition?
- How to transfer between different controllers?

III. Bump Caused by Different Transition Mode

The disturbance caused by mode switching is inherent to dynamic difference of working modes. Even two working points share the same voltage conversion ratio, transient can still occur when switching between the two points. Therefore "voltage conversion ratio" is not a good index for evaluation of dynamic difference. To evaluate the disturbance caused by dynamic difference, a new index *DI* (*Discontinuity Index*) is defined below.

A. Definition of Discontinuity Index (*DI*)

Definition: *For working points A and B share the same steady-state output, DI_{AB} is given by maximum output deviation when open-loop plant changes from A to B.*

DI is a time domain index defined to describe discontinuity of power converter model and no control law is involved. For classical DC-DC converter, every voltage conversion ratio is related to one specific duty ratio, therefore ***DI*** is 0 for classical converter. The case will be different for NIBB.

For generalization of the following discussion, NIBB model in (1) is normalized with per unit value. The per unit voltage, impedance, current and time value are given below:

$$\begin{cases} V_0 = v_o \\ Z_0 = \sqrt{\dfrac{L}{C}} \\ I_0 = \dfrac{V_0}{Z_0} \\ T_0 = 2\pi\sqrt{LC} \end{cases} \tag{4}$$

The resulting average model turns into:

$$\begin{cases} \dfrac{1}{2\pi}\dfrac{di_{Ln}}{dt_n} = d_1 v_{in} - d_2 v_{on} \\ \dfrac{1}{2\pi}\dfrac{dv_o}{dt} = d_2 i_{Ln} - \dfrac{v_{on}}{R_{eqn}} \end{cases} \tag{5}$$

Assuming the initial circuit state are $v_o(0)$ and $i_L(0)$, the initial value of d_2 is d_{2I} and the mode change occurs at t=0, and the duty ratio of S_1 and S_2 are set as d_1 and d_2 respectively. The resulting output voltage can be attained by solving (5).

$$v_o(t) = \frac{w_2\left[v_{on}(0) - \dfrac{d_1}{d_2}v_{in}\right] - 2\pi\left[d_2 i_{Ln}(0) - \dfrac{v_{on}(0)}{R_{eqn}}\right]}{w_2 - w_1} e^{w_1 t} + \frac{-w_1\left[v_{on}(0) - \dfrac{d_1}{d_2}v_{in}\right] + 2\pi\left[d_2 i_{Ln}(0) - \dfrac{v_{on}(0)}{R_{eqn}}\right]}{w_2 - w_1} e^{w_2 t} + \frac{d_1}{d_2}v_{in} \tag{6}$$

Where w_1 and w_2 are circui parameters and given by:

$$w_{1,2} = \pi\left[-\frac{1}{R_{eqn}} \pm \sqrt{\left(\frac{1}{R_{eqn}}\right)^2 - 4d_2^2}\right] \tag{7}$$

Before mode transition, NIBB works in steady-state since A_2 and A_3, B_2 and B_3 have the same voltage conversion ratio. The relation between $v_{o(0)}$ and d_1, d_2 can be expressed as:

$$v_o(0) = \frac{d_1}{d_2} v_i \tag{8}$$

Besides, the relation between d_{2I} and $i_L(0)$ can be derived from steady-state model of (1) as:

$$i_L(0) = \frac{v_o(0)}{d_{2I} R_{eq}} \tag{9}$$

Substituting (8) (9) into (6), the output voltage v_o equals to

$$v_o(t) = \frac{2\pi\left[d_2 i_L(0) - \dfrac{v_o(0)}{R_{eq}}\right]}{(w_2 - w_1)}\left(e^{w_2 t} - e^{w_1 t}\right) + \frac{d_1}{d_2} v_i \tag{10}$$

For NIBB with v_o as the control objective, the normalized *Discontinuity Index* can be presented as:

$$\begin{aligned} DI_n &= \max\left|v_{on}(t) - v_{on}(0)\right| \\ &= \max\left|\frac{\left(e^{w_2 t} - e^{w_1 t}\right)}{(w_2 - w_1)} * \left(\frac{d_2}{d_{2I}} - 1\right) * 2\pi \frac{v_{on}(0)}{R_{eqn}}\right| \end{aligned} \tag{11}$$

It can be seen that ***DI*** is related with d_2 as well as load status R_{eq}. Consider four mode transition scenarios:

- When NIBB changes from A_2 to A_3, D_{2I} equals to D_{max}, d_2 varies from D_{min} to $D_{\max}^2$;
- When NIBB changes from A_3 to A_2, D_{2I} varies from D_{min} to $D_{\max}^2$ and d_2 equals to D_{max};
- When NIBB changes from B_2 to B_3, D_{2I} equals to 1 and d_2 varies from $\dfrac{D_{\min}}{D_{\max}}$ to D_{max};
- When NIBB changes from B_3 to B_2, and D_{2I} varies from $\dfrac{D_{\min}}{D_{\max}}$ to D_{max}, d_2 equals to 1.

A comparison of ***DI*** with different d_2/d_{2I} value for above four scenarios is shown in Fig.4. Here R_{eqn} is the normalized value of R_{eq} listed in Table I. Without loss of generality, D_{max} and D_{min} have been selected as 0.9 and 0.1 respectively.

It can be seen that the different ***DI*** will appear when NIBB transfer from/into *Transition mode*. ***DI*** will be much higher in the former scenario. But one common trend can be noticed: ***DI*** decreases with the increase of d_2/d_{2I}. The same trend also holds for other value of R_{eq}.

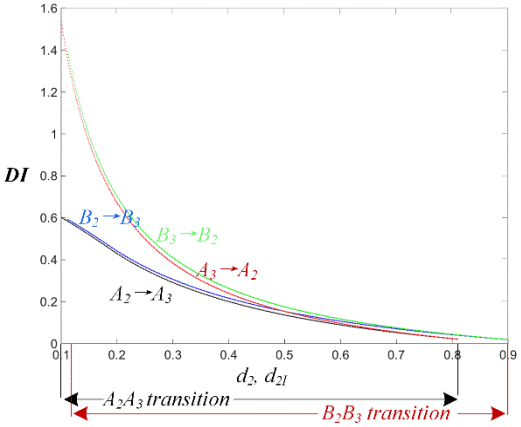

Fig.4 Comparison of ***DI*** in four scenarios with different A_3/B_3

TABLE I. Circuit Parameters

V_o	48V
C	1 mF
L	1mH
R_{eq}	4Ω
f_{sw}	10kHz

B. *Improved Buck/Boost mode for minimum* ***DI***

From above analysis, ***DI*** can be minimized by selecting A_2 and B_2 with maximum d_2 value. For voltage conversion ratio represented as OA_2, maximum d_2 can be attained by selecting working point as A_3. Similarly, for voltage conversion ratio represented as OB_2, the maximum d_2 can be attained by selecting working point as B_3. For ease of implementation, a linear relation between D_1 and D_2 has been defined as transition mode, which is shown as "A_3B_3" in Fig.5. As is shown in Fig.6, the proposed "*Improved Buck/Boost*" mode can achieve lower ***DI*** during mode transition in voltage step-up mode, compared with classical *Buck/Boost mode*. Similar case also holds for voltage step-down mode.

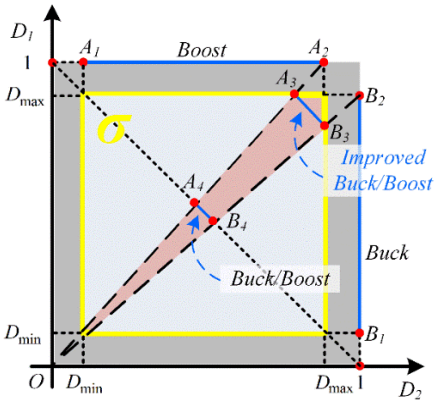

Fig.5 *Improved Buck/Boost mode* as *Transition mode*

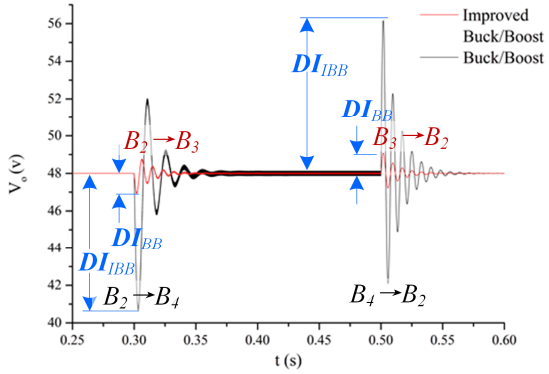

Fig.6 Comparison of ***DI*** during open-loop mode transition in voltage step-up conversion

IV. CURRENT REFERENCE FEED FORWARD COMPENSATION

In above section, the voltage bump caused by open-loop mode transition has been analyzed. For practical implementation, the close-loop control is often essential. For different mode with different dynamic property, the close-loop controllers will be designed for each mode. The resulting control diagram is shown in Fig.7. Following the mode transition logic illustrated in Fig.3, selection of the right mode is decided by comparing input voltage with reference voltage. When working mode changes with the variation of input/output voltage, the inner loop and outer loop controllers will also vary. It is a classical control problem of switching among multiple controllers [8]. The general conclusion is to ensure that all the controllers have the same output, whether it is at work or in idle mode.

Practical implementation of above aim varies from digital controller to analog controller. Take digital controller with PI control as an example, the implementation of PI control can be described as:

$$\begin{cases} PI_N = k_p * err_N + I_N \\ I_N = I_{N-1} + k_i * err_N \end{cases} \qquad (12)$$

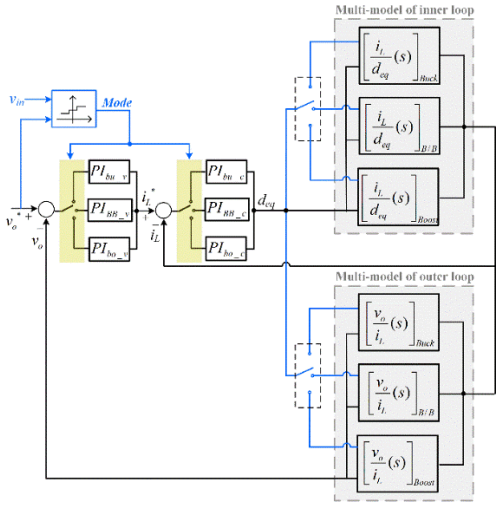

Fig.7 Control diagram for multi-mode operation of NIBB

When PI controller changes from i to j, continuous control output can be ensured with the following logic:

Mode transition detection
(from mode *i* to *j*)
↓
Attain the control output of controller *i* : PI_{N_i}
↓
Reset integral part of controller *j*:
$I_{N\_j} = \left(PI_{N\_i} - k_{P\_j} * err\right) / k_{I\_j}$

However, for NIBB, even when control output keeps continuous during the switching of controllers, output disturbance will still occur, since the dynamic difference of working modes still exists. The condition for smooth output voltage during mode transition can be derived from (1) with:

$$C\frac{dv_o}{dt} = d_2 i_L - \frac{v_o}{R_{eq}} = 0 \qquad (13)$$

The inductor current can be derived from (13) as:

$$i_L = \frac{1}{d_2}\left(\frac{v_o}{R_{eq}}\right) \tag{14}$$

Assuming v_o and R_{eq} keep constant, the discontinuous d_2 value will lead to a gap of i_L deviation. To compensate the gap of inductor current, feed-forward compensation can be used.

Instead of directly measuring the output current i_o, the value can be approximated as current reference before mode transition, i.e.

$$i_{Lj} = \frac{1}{d_{2j}}\left(PI_{V\_i} * d_{2i}\right) \tag{15}$$

Where PI_{V_i} is the control output of outer loop in i mode; d_{2i},d_{2j} are value of d_2 in i and j modes. The control logic of current loop embedded with feed-forward compensation can be presented as:

Mode transition detection
(from mode *i* to *j*)
↓
Attain the control output of controller *i* : PI_{N_i}
↓
Feedforward current reference of *j Mode*:
$PI_{N\_j} = PI_{N\_i} / d_2$
↓
Reset integral part of controller *j*:
$I_{N\_j} = \left(PI_{N\_j} - k_{P\_j} * err\right) / k_{I\_j}$

During the above analysis, time delay of inner control loop has been neglected. It should be noted that the practical response of current loop will not be instant. It is therefore important to decrease ***DI*** at the mode design stage, even with current feed-forward compensation.

V. Numerical and Experimental Verification

In the above analysis, a compound method which consists of *improved buck/boost mode* and *feed-forward bumpless compensation* has been introduced. In evaluation of the proposed method, three combinations of control methods are represented as ①-③ and compared afterwards. Where ①: *Buck/Boost Mode+Classical bumpless control*; ②: *Improved Buck/Boost Mode + Classical bumpless control*; ③ : *Improved Buck/Boost Mode +Feed-forward bumpless control*.

Control design for each mode follows the classical rules: The current loop bandwidth is designed at 1/7 switching frequency with phase margin of 55 degrees; the voltage loop is designed at 1/7 bandwidth of current loop with phase margin of 55 degrees.

As shown in Fig.8, with the increase of input voltage, the working mode of NIBB goes through *Boost* mode, *Buck/Boost* mode or *Improved Buck/Boost* mode and *Buck* mode.

Thanks to the *classical bumpless control*, reference of inductor current I_{Lref} remains unchanged for case ①and case ② during mode transition. A comparison of V_o in ①and ② proved that the *improved Buck/Boost mode* provides decreased voltage disturbance. However, the voltage bump can still be observed in ②. It proves that the *classical bumpless control* is not enough for bumpless operation of NIBB.

For case ③, a step-up of I_{Lref} can be observed during mode transition due to feed-forward current compensation. Compared with case ②, case ③ shows a near bumpless V_o, in support of the proposed *feed-forward bumpless compensation*.

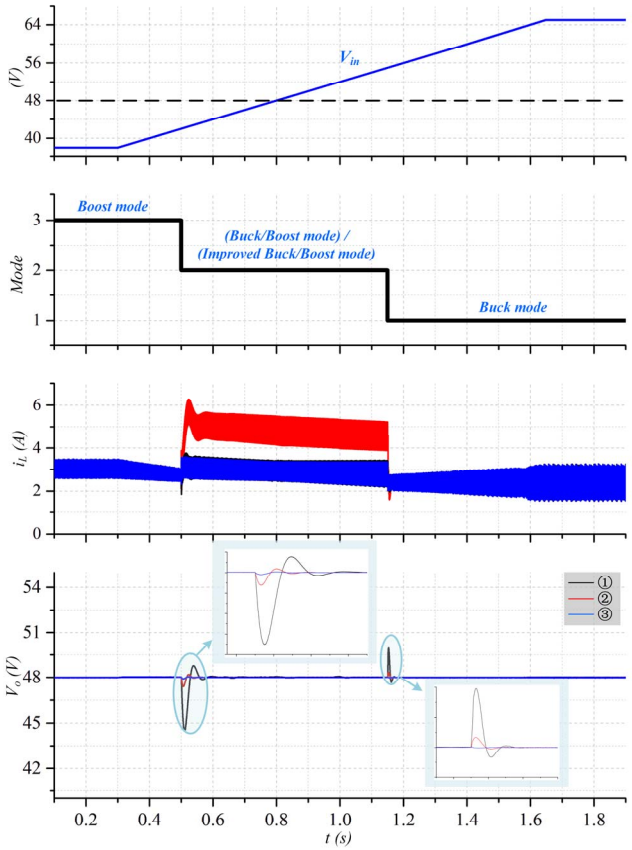

Fig.8 Numerical verification

A prototype of NIBB is also built in verification of the above compound control method. The same three control methods are tested, Where: ① Buck/Boost Mode +Classical bumpless control; ② Improved Buck/Boost Mode +Classical bumpless control; ③ Improved Buck/Boost Mode +Feed-forward bumpless control. A gradual improvement of converter performance from ① to ③ can also be observed, in validation of above analysis.

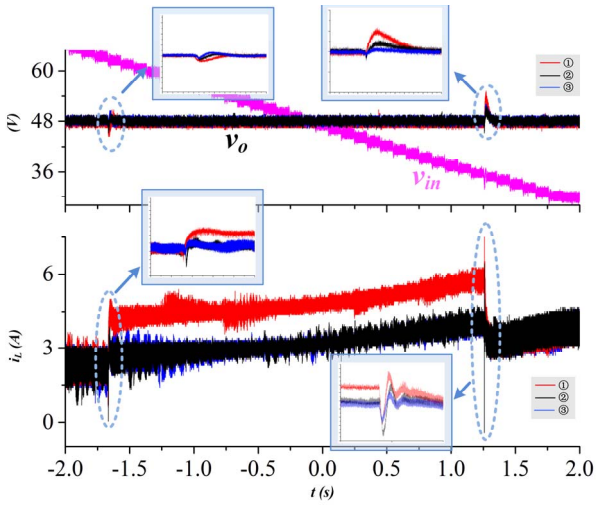

Fig.9 Experimental verification

VI. CONCLUSION

In dealing with the wide voltage range of RES and energy storage devices, NIBB with multi-mode operation has been utilized for efficient power conversion. The transition between multiple modes will introduce extra voltage bump. It involves both open-loop *Transition mode* design as well as switching strategy between close-loop controllers.

In describing the dynamic difference of each mode, *discontinuity index* is defined and serves as design guidance of an *improved buck/Boost mode*. Based on the classical bumpless control, inductor current feed-forward compensation is introduced for control design. A combination of above two techniques gives to bumpless operation of NIBB. The function of each technique is validated by gradual improvement of output performance.

ACKNOWLEDGEMENT

This work is sponsored by the National key research and development program of China: Stability Analysis and Control of Power System Integrating Renewable Energy Generation Bases Delivered By HVDC Transmissions (No. 2017YFB0902000).

REFERENCES

[1] M. Kasper, D. Bortis and J. W. Kolar, "Classification and Comparative Evaluation of PV Panel-Integrated DC–DC Converter Concepts," in*IEEE Transactions on Power Electronics*, vol. 29, no. 5, pp. 2511-2526, May 2014.

[2] M. Anun, M. Ordonez, I. G. Zurbriggen and G. G. Oggier, "Circular Switching Surface Technique: High-Performance Constant Power Load Stabilization for Electric Vehicle Systems," in *IEEE Transactions on Power Electronics*, vol. 30, no. 8, pp. 4560-4572, Aug. 2015.

[3] Jianjun. Ma, M. Zhu, X. Cai and Y. W. Li, "Configuration and operation of DC microgrid cluster linked through DC-DC converter," *2016 IEEE 11th Conference on Industrial Electronics and Applications (ICIEA)*, Hefei, 2016, pp. 2565-2570.

[4] Jianjun. Ma, M. Zhu, J. Zhang and X. Cai, "Improved asynchronous voltage regulation strategy of non-inverting Buck-Boost converter for renewable energy integration," *2015 IEEE 2nd International Future Energy Electronics Conference (IFEEC)*, Taipei, 2015, pp. 1-5.

[5] Jianjun. Ma, M. Zhu, Guanghui Li, Xiuyi Li and X. Cai, "Concept of unified mode control for non-inverting Buck-Boost converter," *2017 IEEE 3rd International Future Energy Electronics Conference and ECCE Asia (IFEEC 2017 - ECCE Asia)*, Kaohsiung, 2017, pp. 1235-1240.

[6] Jianjun Ma, M. Zhu, Guoqing He and X. Cai, "Breaking Performance Limit of Asynchronous Control for Non-inverting Buck Boost Converter," *IECON 2017 - 43th Annual Conference of the IEEE Industrial Electronics Society*, Beijing, 2017.

[7] M. Zhu and F. L. Luo, "Graphical Analytical Method for Power DC–DC Converters: Averaging Binary Tree Structure Representation," in *IEEE Transactions on Power Electronics*, vol. 22, no. 2, pp. 701-705, March 2007.

[8] Åström, Karl Johan, and Tore Hägglund. Advanced PID control. ISA-The Instrumentation, Systems and Automation Society, 2006.

[9] D. C. Jones and R. W. Erickson, "A Nonlinear State Machine for Dead Zone Avoidance and Mitigation in a Synchronous Noninverting Buck–Boost Converter," in *IEEE Transactions on Power Electronics*, vol. 28, no. 1, pp. 467-480, Jan. 2013.

[10] Y. J. Lee, A. Khaligh and A. Emadi, "A Compensation Technique for Smooth Transitions in a Noninverting Buck–Boost Converter," in*IEEE Transactions on Power Electronics*, vol. 24, no. 4, pp. 1002-1015, April 2009.